

# Polyurea Aerogels

Subjects: Polymer Science

Contributor: Nicholas Leventis

The term “aerogel” describes a certain class of low-density solid materials with a high open porosity. Aerogels can be considered to be a subclass of the much broader domain of porous materials; however, they are distinguished from, for example, blown foams, because they are prepared in a completely different manner—namely, by drying wet gels in a way that preserves nearly all of their volume in the final dry form.

Keywords: polyurea ; aerogel ; isocyanate ; amine ; water ; mineral acid ; structure–property relationships ; nanomorphology ; -index

## 1. The Chemistry of Polyurea Aerogels

### 1.1. The Chemistry of the Isocyanate Group

The carbon atom of the isocyanate group,  $\text{--N=C=O}$ , is in the 4+ oxidation state, and is therefore oxidatively stable. The reactivity of the isocyanate group is governed by the electron-withdrawing effects of the oxygen and nitrogen atoms (**Figure 1**), leaving the carbonyl carbon with an enhanced partial positive charge and, thus, susceptible to nucleophilic attack (**Figure 2**).

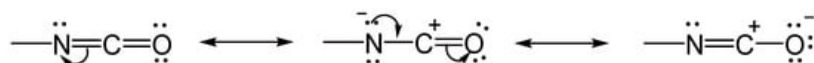


**Figure 1.** Resonance within the isocyanate ( $\text{--N=C=O}$ ) group.

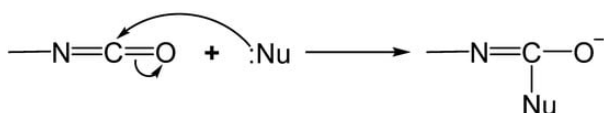


**Figure 2.** Addition of a nucleophile ( $:\text{Nu}$ ) to the isocyanate group.

The reactivity of the isocyanate group ( $\text{--N=C=O}$ ) is modulated by the electron-withdrawing or electron-donating ability of the groups attached to N. Aromatic isocyanates are generally more reactive than aliphatic ones <sup>[1]</sup>. Electron-withdrawing substituents on the aromatic ring enhance the positive charge on the  $\text{--N=C=O}$  carbon even further and, all other factors being equal (for example, steric effects), they increase its reactivity toward nucleophiles <sup>[2]</sup>. Conversely, electron donation due to either resonance (for example,  $\text{MeO--}$ ) or induction (for example,  $\text{CH}_3\text{--}$ ) reduces the reactivity of the  $\text{--N=C=O}$  group. **Figure 3** ranks various aromatic and aliphatic isocyanates in order of their relative reactivity <sup>[1]</sup>.

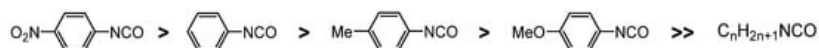


**Figure 3.** The reactivity of the isocyanate group as a function of substitution on the nitrogen of NCO.

As summarized in **Figure 4**, in addition to this straightforward approach to polyurea aerogels, there are two more methods: via reaction of multifunctional isocyanates with water, and with mineral acids. The following subsections of Section 1 and compare these three processes.

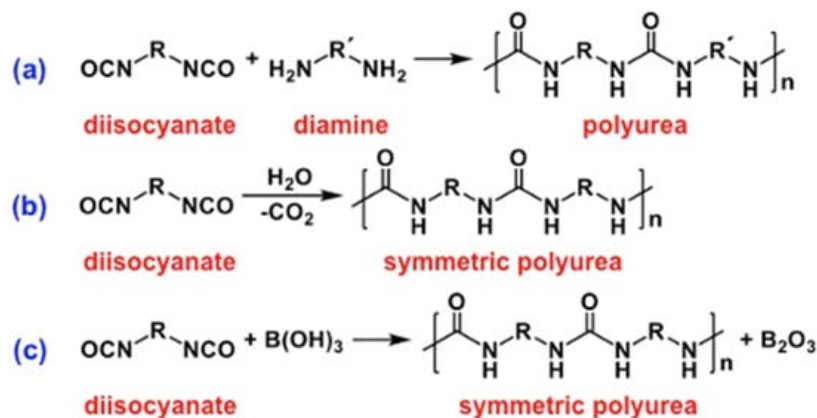


**Figure 4.** The three routes to polyurea aerogels via reaction of multifunctional isocyanates (exemplified here with a diisocyanate) with (a) multifunctional amines, (b) water, and (c) mineral acids (exemplified here with boric acid).

## 1.2. Formation of Polyurea Aerogels via Reaction of the $\text{-N=C=O}$ with Amines

When the nucleophile in **Figure 2** is an amine, the product is a urea (**Figure 5**). The reaction is exothermic, self-catalytic and, typically, fast. The 1,3-proton transfer tautomerization between the two nitrogens in the second step is catalyzed by another molecule of the amine itself acting as a base. Aromatic amines are weaker nucleophiles than aliphatic amines and, therefore, react more slowly than their aliphatic counterparts [3].

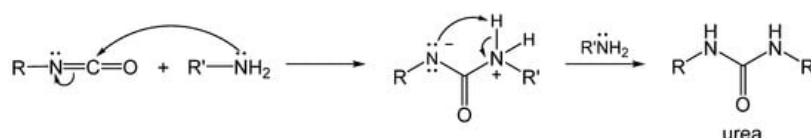


**Figure 5.** Urea formation via reaction of an isocyanate with an amine.

Ureas, in turn, acting as *N*-based nucleophiles, can attack excess isocyanate to yield biurets (**Figure 6**). The nucleophilicity of ureas toward  $\text{-N=C=O}$  is low, and the reaction takes place at higher temperatures (100–150 °C) [4]. Nevertheless, the formation of biurets serves as a crosslinking mechanism for polyurea.

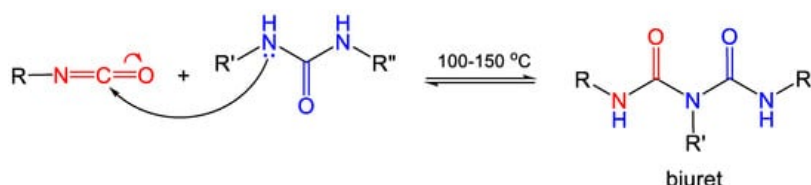


**Figure 6.** The reaction of isocyanates with ureas to form biurets. The arrows show the initial nucleophilic attack. The overall reaction involves several intermediates. Color coding is used for tracking purposes.

Desmodur N3200 from Covestro LLC—a triisocyanate that has been used extensively in the synthesis of polyurea and polyurea-crosslinked oxide aerogels—is a biuret derived from hexamethylene diisocyanate (HDI) (**Figure 7**) [5].

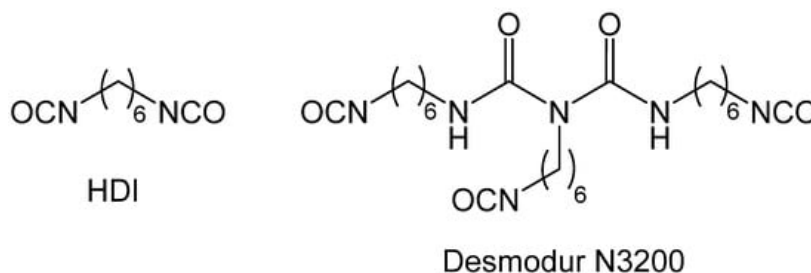


**Figure 7.** Hexamethylene diisocyanate (HDI) and the primary component of Desmodur N3200 (a biuret derivative of HDI), manufactured by Covestro LLC (Pittsburgh, PA, USA).

## 1.3. Formation of Polyurea Aerogels via Reaction of $\text{-N=C=O}$ with Water

Water acting as a nucleophile attacks the isocyanate carbonyl to yield a carbamic acid, which is unstable and decomposes into an amine and carbon dioxide (**Figure 8**). The hydrolytic reaction leading to the carbamic acid is slow, and in practice is usually catalyzed by non-nucleophilic tertiary amines, e.g., triethylamine ( $\text{Et}_3\text{N}$ ). The primary amine

formed by decomposition of the carbamic acid reacts rapidly with a second, unreacted isocyanate, as shown in **Figure 5**, forming a symmetric urea [6][7]. Since the sequence of reactions in **Figure 5** and **Figure 8** bypasses the use of extraneous amines for the synthesis of ureas, it represents a cost-effective alternative to the process of **Figure 5** for synthesizing symmetric polyurea aerogels. By the same token, however, the reaction sequence of **Figure 5** and **Figure 8** is not an atom-efficient process, as a carbon atom is lost as CO<sub>2</sub>. Therefore, this reaction pathway is not typically used for the synthesis of bulk polyurea. Industrially, a small amount of water is often added deliberately as a foaming agent during preparation of bulk polyurethane foams [8]. When it comes to the synthesis of polymeric aerogels, however, loss of CO<sub>2</sub> is not a deterrent, because aerogels require only small amounts of monomers, and the cost of the mass loss due to CO<sub>2</sub> evolution is just a small fraction of the overall cost. Although CO<sub>2</sub> evolution during polyurea aerogel synthesis can potentially result in unwanted voids in the resulting monolithic parts, in practice this has not been reported as a problem.

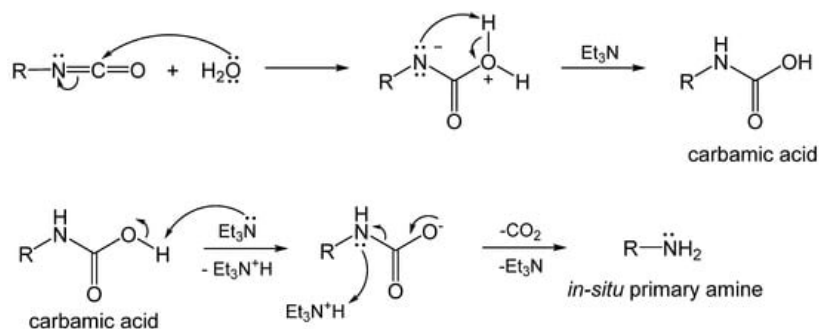


**Figure 8.** In situ formation of amines from the reaction of isocyanates with water. The 1,3-proton transfer tautomerization of the first step is catalyzed by non-nucleophilic tertiary amines such as Et<sub>3</sub>N. In the second step, Et<sub>3</sub>N first undergoes an acid–base reaction with carbamic acid. The resulting carbamate expels CO<sub>2</sub>, while also taking back a proton from [Et<sub>3</sub>NH]<sup>+</sup> to form an amine.

In addition to Desmodur N3200 (**Figure 7**), other multifunctional isocyanates that have been used in polyurea aerogel synthesis include the two triisocyanates shown in **Figure 9**.

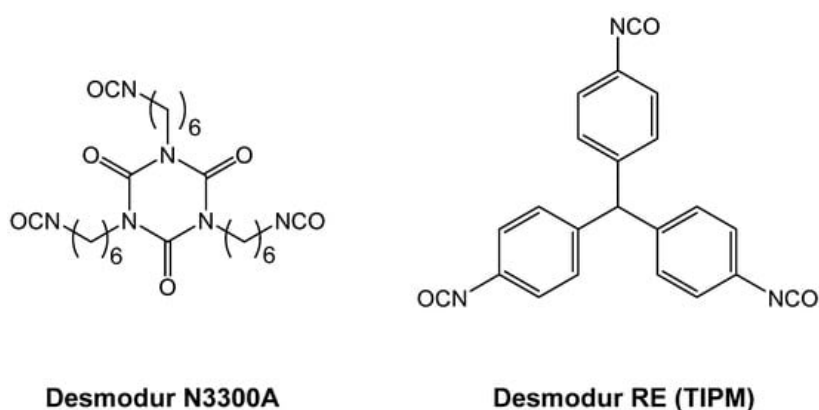


**Figure 9.** Commercially available triisocyanates (from Covestro LLC) that have been used extensively for making polyurea aerogels via reaction with water. Desmodur N3300A: an isocyanate trimer of hexamethylene diisocyanate (HDI, see **Figure 7**), supplied as a pure compound. Desmodur RE: Tris(4-isocyanatophenyl)methane, a rigid aromatic triisocyanate, usually abbreviated as TIPM, supplied as an ethyl acetate solution.

#### 1.4. Formation of Polyurea Aerogels via Reaction of –N=C=O with Mineral Acids

The reaction of isocyanates with mineral acids to yield polyurea aerogels was first reported in 2016 [9], and is summarized in the most general terms in **Figure 10**. This discovery stemmed from an effort to prepare boramic aerogels by reproducing a procedure reported in a 1962 patent [10]. According to that procedure, boramides (for example, materials with –B–NH– linkages) could be prepared via reaction of isocyanates with boric acid, in analogy to the well-understood reaction of isocyanates with carboxylic acids, yielding amides [11][12]. What was obtained instead was a pure polyurea aerogel. The proposed mechanism starts with the formation of the carbamic–boric anhydride adduct, in analogy to the reaction of –COOH with –N=C=O. The carbamic–boric anhydride adduct can then react with another molecule of the same kind (**Figure 11**, Route 1), or with an isocyanate (**Figure 11**, Route 2). The two routes converge to a common intermediate (**Figure 11**, Int-1) that reacts with another molecule of boric acid. The next intermediate (Int-2) rearranges itself into urea and boric oxide (B<sub>2</sub>O<sub>3</sub>: the anhydride of boric acid). Overall, the isocyanate/mineral acid system behaved as if it proceeded along an established pathway in the reaction of –COOH and –N=C=O, but stopped at the intermediate

urea/anhydride stage.  $B_2O_3$  can be removed completely during post-gelation washes, leaving behind a pure polyurea wet gel, which is dried into an aerogel [9].

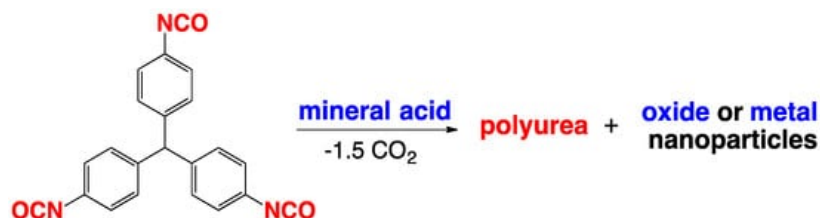


**Figure 10.** General gelation pathway from reaction of a triisocyanate (Desmodur RE; see **Figure 9**) with mineral acids.

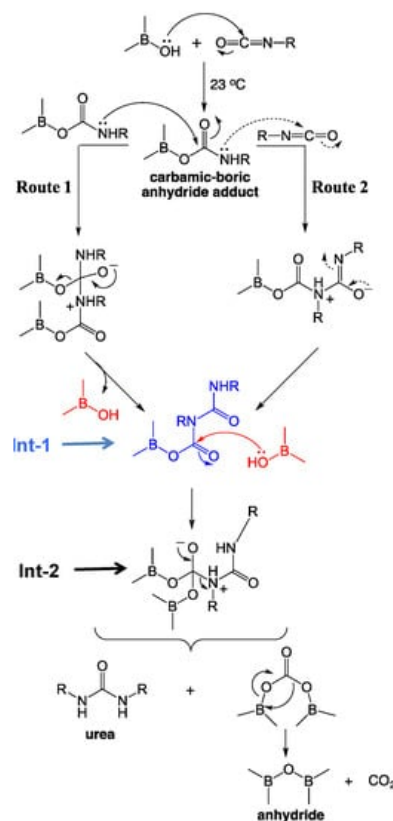


**Figure 11.** Proposed mechanism for the formation of urea from isocyanate and  $H_3BO_3$  (Note, boric acid is used here as a proxy for any of several other possible mineral acids).

This new pathway to polyurea aerogels is quite general; in addition to  $H_3BO_3$ , reaction of the same triisocyanate with  $H_3PO_4$ ,  $H_3PO_3$ ,  $H_2SeO_3$ ,  $H_6TeO_6$ ,  $H_5IO_6$ , and  $H_3AuO_3$  always yielded the same polyurea aerogel; however, while the anhydride side product from the reaction with  $H_3BO_3$  (that is  $B_2O_3$ ) could be washed off easily from the porous structure of the wet gels, the other oxides were insoluble, and remained as nanodispersed dopants in the final polyurea aerogels, as well as in the corresponding carbon aerogels derived from them by pyrolysis. An interesting exception was gelation with auric acid where, due to the instability of the oxide, both the corresponding polyurea aerogel and the derived carbon aerogel were doped with nanodispersed Au nanoparticles.

## 2. Translating the Polymerization Chemistry into Aerogels

### 2.1. The Gelation Process and Nanomorphology

The polymerization processes described in Section 1 turn soluble monomers into insoluble polymers that comprise the skeletal framework of the aerogel. The morphology of the skeletal framework of polyurea aerogels can be very diverse, even within the well-defined chemical composition of a specific polymer. This morphological diversity arises from parameters such as the molecular structure of the monomers (for example, aromatic versus aliphatic, rigid versus flexible, difunctional versus polyfunctional, the functional group density at the monomer molecular level), the solubility properties of the medium (for example, polarity, ability to develop dispersion forces, and hydrogen bonding), the concentrations of the monomers and the catalyst, and the gelation temperature.

The formation of an insoluble polymer means phase separation, which can be of either solid primary particles (**Figure 12**, left branch), or of an oily phase of insoluble oligomers (**Figure 12**, right branch) [13][14][15]. In the first case, the size of the primary particles decreases as the functionality and functional-group density of the monomers increases, leading quickly to a highly crosslinked, insoluble polymer. This has been demonstrated well with poly(urethane acrylate) aerogels derived from trifunctional versus nine-functional (nonafunctional) star and dendritic monomers, respectively; the two types of monomers, made using the same rigid aromatic triisocyanate core, yielded primary particles with radii equal to 17 nm versus 7 nm, respectively [16][17].

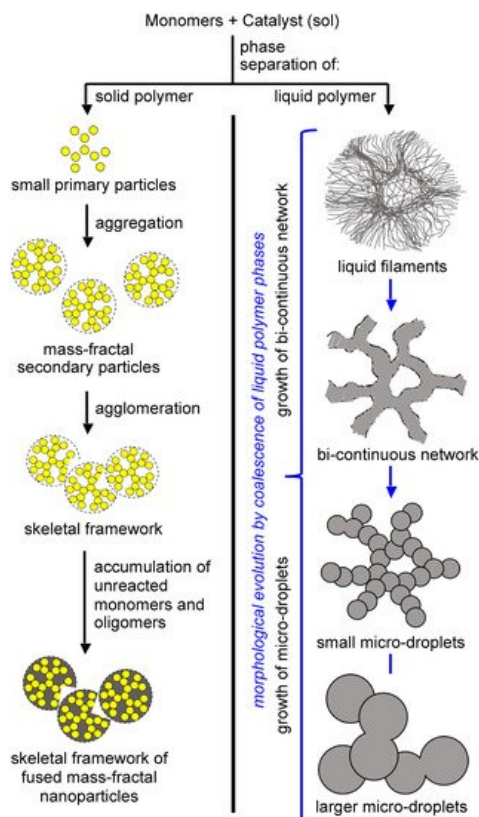


**Figure 12.** Phase separation and growth processes involved in the formation of the skeletal network of gels.

Phase-separated primary particles move randomly in the sol, and upon collision with one another they may become chemically connected via reaction with yet-unreacted surface functional groups inherited from the monomers. If the reaction is fast (and, thus, the sticking probability for each collision is high), the kinetics of network growth are limited only by diffusion, and the process is referred to as diffusion-limited aggregation. Such aggregates are mass fractal objects [15], and their size is limited by the fact that their density falls rapidly with distance from the nucleation point at their center; this is to say that beyond a certain size there is not enough mass in their outer “layers” to support further growth. These fractal aggregates of primary particles are referred to as secondary particles. On geometric grounds, the pore sizes within secondary particles are in the same order as the primary particles, and typically they fall in the mesopore range (2–50 nm). Secondary particles also randomly walk, albeit more slowly, eventually being connected to one another via chemical bonding to form higher aggregates. The liquid sol turns into a solid gel once secondary particles, or higher aggregates, have formed a continuous interconnected three-dimensional path spanning the entire volume of the liquid within a mold. At that point, assuming that all monomers have been consumed, the skeletal network consists of interconnected secondary particles or higher aggregates. Experimentally, primary particles are identified, and their size is estimated using small-angle X-ray or neutron-scattering data (SAXS or SANS, respectively); alternatively, the primary particle size is calculated from skeletal density and  $N_2$  sorption data via  $r = 3/(\rho_s \times \sigma)$ , where  $r$  is the particle radius,  $\rho_s$  is the skeletal density from He pycnometry; and  $\sigma$  is the BET surface area from  $N_2$  sorption porosimetry. The primary particle size obtained via the two methods should be roughly equal. This situation is very common with oxide aerogels, and is also encountered with several polyurea aerogels. If unreacted monomers or soluble oligomers remain in the pores after gelation, these species eventually find their way onto the protoskeletal framework, where they can accumulate via reaction with still-live functional groups on the surface of the framework. Eventually, accumulation of monomers and/or oligomers fills the void space within the secondary particles and, experimentally, the particle size calculated from skeletal density and  $N_2$  sorption data reflects a size closer to that of the secondary particles as determined via SAXS or SANS. Under SEM, these structures appear as if they consist of random assemblies of particles, with a layer of polymer cast over the entire network [16]. The topography of such an arrangement actually resembles that of polymer-crosslinked oxide aerogels, in which silica primary particles are embedded within a crosslinker-derived polymer that fills the space within the

aerogel's secondary particles <sup>[18][19]</sup>. Comparisons of particle sizes determined from skeletal density/N<sub>2</sub> sorption data and SAXS have proven useful in understanding the growth mechanisms underlying the formation of polymeric aerogels in general.

An interesting variation of the theme described in the previous paragraph is encountered when, within a series of aerogel samples of variable density, the particle size determined from skeletal density/N<sub>2</sub> sorption data matches the primary particle size from SAXS for high-density aerogels, but diverges—sometimes by orders of magnitude—at lower densities. This type of density-dependent trend is attributed to a sol-concentration-dependent gelation mechanism, and is typically accompanied by obvious morphological changes in SEM and large changes in the BET surface area <sup>[20]</sup>.

Phase separation of oligomers as an oily liquid (**Figure 12**, right branch) occurs with large flexible monomers with low functional-group density. The “oil” continues to react internally until it is solidified (arrested). Depending on the speed of solidification and the properties of the medium, the structural diversity that can be generated via this process can be extremely broad. For example, the oily phase may start out as thin, hair-like filaments that evolve into small droplets embedded within fibers; among other possibilities, the latter morphology may evolve into large particles with or without fibers emanating from their surface. By choosing the right monomers and adjusting the reaction rate (for example, via adjustment of monomer concentration, or by using an appropriate catalyst), any skeletal framework with these morphologies can be “frozen” (kinetically trapped) in place before it has time to evolve into the next step. Polyurea aerogels are an extremely versatile class of materials that enable observation and, in some cases, design of those morphologies in the final products. For example, **Figure 13** shows a very large array of nanostructures, all with identical chemical composition, prepared via reaction of Desmodur N3300A (see **Figure 9**) and water (see **Figure 4b**) in various solvents at different monomer concentrations.

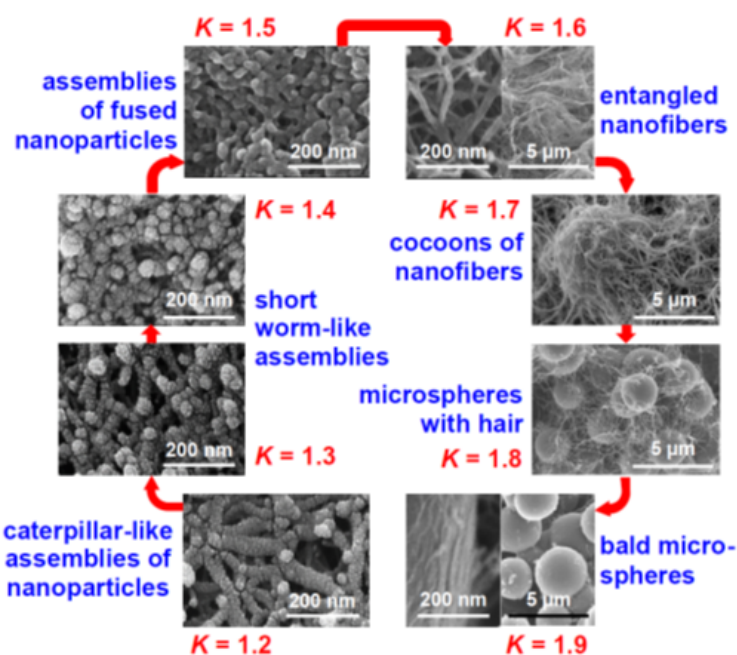


**Figure 13.** Eight (8) nanomorphology groups identified from 188 formulations of Desmodur N3300A/water-derived polyurea aerogels prepared using 8 different solvents (i.e., acetone, acetonitrile, nitromethane, propylene carbonate, THF, DMF, 2-butanone, and ethyl acetate). *K*-index is defined as the ratio of the water contact angle to the percentage of porosity for a given material. Each morphological group shown in this figure was associated with a unique *K*-index value <sup>[21]</sup>.

These skeletal morphologies of **Figure 13** translate directly into a wide range of surface areas, texture-induced hydrophobicity, and diverse mechanical properties that include superelasticity and shape-memory effects.

## 2.2. Molding, form Factors, and the Drying Process

Nanostructured polyurea aerogels can be produced in various form factors, ranging from monoliths to particles. Shaped monoliths are produced by pouring the polyurea sol into suitable molds and allowing it to gel. Irregular polyurea aerogel particles are produced by stirring the sol vigorously until gelation. Particles in the form of spherical millimeter-size beads may be formed via a dripping method. The use of surfactants for the synthesis of micron-size beads, or of 3D printing—as was reported recently for giving complicated shapes to structurally related polyurethane aerogels <sup>[22]</sup>—have not yet been reported with polyurea aerogels.

Drying in most cases has been carried out using supercritical fluid (SCF) CO<sub>2</sub>. Polyurea aerogels have also been produced via freeze-drying by replacing the pore-filling solvent with *tert*-butanol, followed by freezing and subsequent sublimation [23][24]. The freeze-drying process provides easier access to large monolithic panels than supercritical drying; however, the process parameters seem to have a significant influence on the properties of the resulting polyurea aerogels.

---

## References

1. Saunders, J.H.; Frisch, K.C. Polyurethane Chemistry and Technology: Chemistry; Interscience Publishers: Hoboken, NJ, USA, 1964; pp. 63–118.
2. Stevens, M.P. Polymer Chemistry. An Introduction; Oxford University Press: New York, NY, USA, 1990.
3. Davis, T.L.; Ebersole, F. Relative velocities of reaction of amines with phenyl isocyanate. *J. Am. Chem. Soc.* 1934, 56, 885–886.
4. Neumann, W.; Fischer, P. Carbodiimide aus Isocyanaten. *Angew. Chem.* 1962, 74, 801–806.
5. Available online: <https://coatings.specialchem.com/product/r-covestro-desmodur-n-3200> (accessed on 26 February 2022).
6. Wicks, Z.W., Jr.; Jones, F.N.; Pappas, S.P.; Wicks, D.A. Organic Coatings, Science & Technology, 3rd ed.; Wiley-Interscience: Hoboken, NJ, USA, 2007.
7. Odian, G. Principles of Polymerization; Wiley-Interscience: New York, NY, USA, 2004.
8. Dodge, J. Polyurethanes and Polyureas. In *Synthetic Methods in Step-Growth Polymers*; Rogers, M.E., Long, T.E., Eds.; Wiley: New York, NY, USA, 2003; pp. 197–263.
9. Leventis, N.; Sotiriou-Leventis, C.; Saeed, A.M.; Donthula, S.; Majedi Far, H.; Rewatkar, P.M.; Kaiser, H.; Robertson, J.D.; Lu, H.; Churu, G. Nanoporous polyurea from a triisocyanate and boric acid: A paradigm of a general reaction pathway for isocyanates and mineral acids. *Chem. Mater.* 2016, 28, 67–78.
10. Aries, R.S. Polymers from Boric Acid and Organic Diisocyanates. U.S. Patent No 2,945,841, 19 July 1960.
11. Xiao, H.; Xiao, H.X.; Frisch, K.C.; Malwitz, N. Kinetic studies of the reactions between isocyanates and carboxylic acids. *High Perform. Polym.* 1994, 6, 235–239.
12. Sorenson, W.R. Reaction of an isocyanate and a carboxylic acid in dimethyl sulfoxide. *J. Org. Chem.* 1959, 24, 978–980.
13. Trappe, V.; Prasad, V.; Cipelletti, L.; Segre, P.N.; Weitz, D.A. Jamming phase diagrams for attractive particles. *Nature* 2001, 411, 772–775.
14. Lu, P.J.; Zaccarelli, E.; Ciulla, F.; Schofield, A.B.; Sciortino, F.; Weitz, D.A. Gelation of particles with short-range attraction. *Nature* 2008, 459, 499–503.
15. Rouwhorst, J.; Ness, C.; Stoyanov, S.; Zacccone, A.; Schall, P. Nonequilibrium continuous phase transition in colloidal gelation with short-range attraction. *Nature Commun.* 2020, 11, 3558.
16. Bang, A.; Buback, C.; Sotiriou-Leventis, C.; Leventis, N. Flexible aerogels from hyperbranched polyurethanes: Probing the role of molecular rigidity with poly(urethane acrylates) versus poly(urethane norbornenes). *Chem. Mater.* 2014, 26, 6979–6993.
17. Papastergiou, M.; Kanellou, A.; Chriti, D.; Raptopoulos, G.; Paraskevopoulou, P. Poly(urethane-acrylate) aerogels via radical polymerization of dendritic urethane-acrylate monomers. *Materials* 2018, 11, 2249.
18. Mohite, D.P.; Larimore, Z.J.; Lu, H.; Mang, J.T.; Sotiriou-Leventis, C.; Leventis, N. Monolithic hierarchical fractal assemblies of silica nanoparticles cross-linked with polynorbornene via ROMP: A structure-property correlation from molecular to bulk through nano. *Chem. Mater.* 2012, 24, 3434–3448.
19. Mohite, D.P.; Mahadik-Khanolkar, S.; Luo, H.; Lu, H.; Sotiriou-Leventis, C.; Leventis, N. Polydicyclopentadiene aerogels grafted with PMMA: II. Nanoscopic characterization and origin of macroscopic deformation. *Soft Matter* 2013, 9, 1531–1539.
20. Chidambareswarapattar, C.; McCarver, P.M.; Luo, H.; Lu, H.; Sotiriou-Leventis, C.; Leventis, N. Fractal multiscale nanoporous polyurethanes: Flexible to extremely rigid aerogels from multifunctional small molecules. *Chem. Mater.* 2013, 25, 3205–3224.
21. NEW REFERENCE: Taghvaei, T.; Donthula, S.; Rewatkar, P.M.; Majedi Far, H.; Sotiriou-Leventis, C.; Leventis, N. K-index: Descriptor, predictor, and correlator of complex nanomorphology to other material properties. *ACS Nano* 2019, 13, 3677–3690.

22. Malakooti, S.; ud Doulah, A.B.M.S.; Ren, Y.; Kulkarni, V.N.; Soni, R.U.; Edlabadkar, V.A.; Zhang, R.; Vivod, S.L.; Chariklia Sotiriou-Leventis, C.; Leventis, N.; et al. Meta-aerogels: Auxetic shape-memory polyurethane aerogels. *ACS Appl. Polym. Mater.* 2021, 3, 5727–5738.
  23. Członka, S.; Bertino, M.F.; Kośny, J.; Shukla, N. Freeze-drying method as a new approach to the synthesis of polyurea aerogels from isocyanate and water. *J. Sol-Gel Sci. Technol.* 2018, 87, 685–695.
  24. Steiner, S.A., III; Griffin, J.S.; Wunsch, B.H.; Schneider, J.N. Systems and Methods for Producing Aerogel Materials. U.S. Patent No 10,563,035 B2, 18 February 2020.
- 

Retrieved from <https://encyclopedia.pub/entry/history/show/50990>